Some Applications of Direct Adaptive Control to Large Structural Systems

I. Bar-Kana* and H. Kaufman†
Rensselaer Polytechnic Institute, Troy, New York

Direct multivariable model reference adaptive control applications are considered with three representative examples of large structural systems such as beams, plates, and frames. Such applications have in the past been shown to be feasible for multivariable systems provided that there exists a constant feedback gain matrix such that the resulting input-output transfer function is (simply) positive real. This sufficient condition is satisfied in large structural systems using velocity feedback when the actuators and the sensors are collocated. When velocity and position feedback are used to allow position control of the structure, the positivity condition can be satisfied if some amount of damping is assumed for the structure. In this paper, applications are considered for regulation and for position and velocity control. All the systems used in examples are totally undamped, and in some examples, the actuators and the sensors are not perfectly collocated, thus not satisfying the positive realness conditions. Simulation results show satisfactory behaviors for both regulation and servo-following.

Introduction

THE need for adaptive control of large structural systems (LSS) arises because of ignorance of the critical parameters' value as well as of their operating environments. One particular adaptive algorithm which seems suitable for LSS is the direct multivariable model reference adaptive control (DMMRAC) algorithm developed in Ref. 1 and extended in Refs. 2-4. The reference model used with this algorithm is defined to incorporate the design specifications but it is quite free otherwise and need not be of the same order as the plant.

It was shown that a sufficient condition to guarantee the stability of the adaptive system is the existence of a constant feedback gain matrix (not needed for implementation) such that the resulting input-output transfer function is (simply rather than strictly) positive real.[2]

This sufficient condition is satisfied in LSS only if velocity feedback is used, when the sensors and actuators are collocated even if the structure is totally undamped. If velocity plus scaled position feedback is used, then positive realness is satisfied if there exists sufficient damping and if the sensors and the actuators are again collocated.

In this paper, applications are considered with regulation and position control using either velocity or velocity plus scaled position feedback. Examples with sensors and actuators not perfectly collocated are also considered. All the examples use totally undamped structures, even though in some cases the positive realness condition is not necessarily satisfied.

The performance of the controller is evaluated for three representative examples of large structural systems and is shown to be quite acceptable, even though no a priori information about the controlled plant is used for implementation.

Problem Formulation

The controlled plant is represented by

$$\dot{x}_p(t) = A_p x_p(t) + B_p u_p(t) \tag{1}$$

$$y_p(t) = C_p x_p(t) \tag{2}$$

and the plant output is required to follow the output of the reference model

$$\dot{x}_m(t) = A_m x_m(t) + B_m u_m(t) \tag{3}$$

$$y_m(t) = C_m x_m(t) \tag{4}$$

where it is possible to have

$$\dim(x_p) \geqslant \dim(x_m)$$

We represent the input command $u_m(t)$ as the output of a command generating system of the form,

$$\dot{v}_m(t) = A_v v_m(t) \tag{5}$$

$$u_m(t) = C_v v_m(t) \tag{6}$$

The representation, Eqs. (5) and (6), is needed only for the subsequent analysis. The matrices A_v and C_v are unknown and only measurement of the input $u_m(t)$ is permitted. When the plant output follows the output of the model the plant is assumed to be moving along some "ideal trajectories" of the form

$$x_p^*(t) = X_{11} x_m(t) + X_{12} v_m(t) \tag{7}$$

The state error is defined as

$$e_x(t) = x_p^*(t) - x_p(t) \tag{8}$$

and the output error is then

$$\begin{aligned} e_y(t) &= y_m(t) - y_p(t) = C_m x_m(t) - C_p x_p(t) \\ &= C_m x_m(t) - C_p x_p^*(t) = C_p e_x(t) \end{aligned} \tag{9}$$

The adaptive algorithm generates the following plant control[1]:

$$u_p(t) = K(t) r(t) = K_e(t) e_y(t) + K_x(t) x_m(t) + K_u(t) u_m(t) \tag{10}$$

Submitted April 5, 1983; revision received July 26, 1983.

*Research Assistant, Electrical, Computer, and Systems Engineering Department.

†Professor, Electrical, Computer, and Systems Engineering Department.

where

$$K(t) \triangleq [K_e(t) \;\; K_x(t) \;\; K_u(t)] \tag{11}$$

$$r^T(t) \triangleq [e_y^T(t) \;\; x_m^T \;\; u_m^T(t)] \tag{12}$$

and

$$K(t) = K_p(t) + K_I(t) \tag{13}$$

$$K_p(t) = e_y(t) r^T \bar{T} \tag{14}$$

$$\dot{K}_I(t) = e_y(t) r^T(t) T \tag{15}$$

T and $\bar{T}$ are positive definite adaptation gain matrices. The differential equation of the state error is then

$$\begin{aligned} \dot{e}_x(t) = {} & (A_p - B_p K_e(t) C_p) e_x(t) - B_p [K_x(t) x_m(t) \\ & + K_u(t) u_m(t) + K_e(t)(C_m x_m(t) - C_p x_p^*(t))] \\ & - [(A_p X_{11} - X_{11} A_m) x_m(t) \\ & + (A_p X_{12} - X_{12} A_v - X_{11} B_m C_v) v_m(t)] \end{aligned} \tag{16}$$

The following quadratic Lyapunov equation was used[4] to prove stability for Eqs. (15) and (16):

$$V = e_x^T(t) P e_x(t) + \operatorname{tr}[S(K_I(t) - \tilde{K}) T^{-1} (K_I(t) - \tilde{K})^T S^T] \tag{17}$$

where

$$\tilde{K} = [\tilde{K}_e \;\; \tilde{K}_x \;\; \tilde{K}_u] \tag{18}$$

and S is an arbitrary nonsingular matrix.

It can be shown that the derivative of V is[4]:

$$\dot{V}(t) = g_1(t) + g_2(t) + g_3(t) \tag{19}$$

where

$$g_1(t) = e_x^T [P(A_p - B_p \tilde{K}_e C_p) + (A_p - B_p \tilde{K}_e C_p)^T P] e_x(t) \tag{20}$$

$$g_2(t) = -2 e_y^T(t)(S^T S) e_y(t) r^T(t) \bar{T} r(t) \tag{21}$$

$$\begin{aligned} g_3(t) = {} & 2[r^T(t) \bar{T} r(t) e_y^T(t)(S^T S)(C_p X_{11} - C_m) \\ & + r^T(t)(K_I(t) - \tilde{K})(S^T S)(C_p X_{11} - C_m) \\ & - e_x^T(t) P B_p (K_{Ie}(t) - \tilde{K}_e)(C_p X_{11} - C_m) \\ & - e_x^T(t) P (A_p X_{11} - X_{11} A_m + B_p \tilde{K}_x)] e^{A_m t} \delta_0 \end{aligned} \tag{22}$$

A sufficient condition for boundedness of all values involved in the adaptation process and for the asymptotically perfect model following is the existence of some positive definite matrix P and of some constant gain matrix $\tilde{K}_e$ (not needed for implementation) such that

$$P B_p = C_p^T (S^T S) \tag{23}$$

$$P(A_p - B_p \tilde{K}_e C_p) + (A_p - B_p \tilde{K}_e C_p)^T P \leq 0 \tag{24}$$

Conditions in Eqs. (23) and (24) are equivalent to requiring that the closed-loop input-output transfer function

$$Z(s) = C_p (sI - A + B_p \tilde{K}_e C_p)^{-1} B_p \tag{25}$$

be (simply rather than strictly) positive real.

If the condition of Eq. (24) is satisfied, then $g_1(t)$ in Eq. (19) is negative semidefinite. By applying the Gronwall-Bellman inequality[5] to Eq. (19), it can be shown[4] that all state errors, $e_x(t)$, gains, $K_I(t)$, and output errors, $e_y(t)$, are bounded. In that case

$$g_3(t) \to 0 \quad \text{as} \quad t \to \infty$$

Since $g_2(t)$ is negative definite with respect to $e_y(t)$, subsequent application of LaSalle's Invariance Principle[6] shows that the system reaches its equilibrium state for $e_y(t) \to 0$ as $t \to \infty$.

Considering that the above conditions, Eqs. (23) and (24), are sufficient but not necessary for insuring stability, the DMMRAC will be used in the following cases, which include systems that are not necessarily positive real:

1) Velocity feedback only, actuators and sensors collocated, positive real conditions satisfied.

2) Velocity feedback only, actuators and sensors not perfectly collocated, positive real conditions satisfied.

3) Velocity plus scaled position feedback, actuator and sensor collocated, positive real condition, Eq. (24), not satisfied.

4) Velocity plus scaled position feedback, actuators and sensors not perfectly collocated. Positive real condition, Eq. (24), not satisfied.

It is of interest to comment here that the subsequent applications of adaptive control require minimal information regarding system structure. For example, in order to guarantee asymptotic stability it must be a priori known that the process is indeed output stabilizable and that it will, for some feedback gain, (not needed for implementation) be positive real. All the structures with collocated actuators and sensors as considered in the next section satisfy these conditions, and as a result the output errors and state norms are shown under regulation to approach zero.

Although the issue of noncollocated sensors and actuators is addressed by simulation in the first example, a complete analysis of this effect, along with the influence of disturbances and sensor and actuator dynamics, is a topic of current research which is addressed in the Conclusion.

Application of DMMRAC in Large Structural Systems

DMMRAC algorithms are used to design controllers for three different structures: an eight-state beam,[8] a 24-state plate,[9] and a 30-state truss.[10] All the structural models are totally undamped.

The large structural model used in the subsequent simulations can be defined by the following matrices

$$A_p = \begin{bmatrix} 0 & I \\ -\Lambda & -2z\Lambda^{1/2} \end{bmatrix} \tag{26}$$

$$B_p = \begin{bmatrix} 0 \\ B_2 \end{bmatrix} \tag{27}$$

where

$$\Lambda = \operatorname{diag}(\lambda_1, \lambda_2, \ldots, \lambda_n); \qquad \lambda_1 \leq \lambda_2 \ldots \leq \lambda_n \tag{28}$$

and where z is the damping coefficient. If only velocity output is measured, then

$$C_p = [0 \;\; C_2] \tag{29}$$

If velocity plus scaled position is measured, then

$$C_p = [\alpha C_2 \quad C_2] \tag{30}$$

The reference model is a reduced order model described by

$$A_m = \begin{bmatrix} 0 & I \\ -\Lambda_m & -2z_m\Lambda_m^{1/2} \end{bmatrix} \tag{31}$$

$$B_m = \begin{bmatrix} 0 \\ B_m \end{bmatrix} \tag{32}$$

$$C_m = [\alpha C_{m2} \quad C_{m2}] \tag{33}$$

It can be shown that the positivity conditions can be satisfied with velocity control, Eq. (29), if the sensors and the actuators are collocated, i.e., if

$$B_2 = \beta C_2^T \tag{34}$$

When position control is desired and thus, velocity plus scaled position is measured, per Eq. (28), the positive realness conditions can only be satisfied if some amount of damping is assumed to exist ($z>0$), and in that case the scaling of the position is limited[4,7] by

$$\alpha \leq \min(z\sqrt{\lambda_i}, z^{-1}\sqrt{\lambda_i}) \tag{35}$$

However, in the subsequent computer simulations the plants are all totally undamped ($z=0$); despite this, a feedback signal equal to position plus velocity (i.e., $\alpha=1$) was considered for use in the adaptive algorithm.

Eighth-Order Regulation and Servo-Following Example

An undamped eighth-order, two-output representation of a normalized 1 m simply supported beam[7] was considered for adaptive controller design. The beam is defined by the matrices:

$$\Lambda = \text{diag}[\pi^4 \ (2\pi)^4 \ (3\pi)^4 \ (4\pi)^4]$$

Two actuators and two sensors were correspondingly collocated at $d_1 = 0.29$ and $d_2 = 0.84$, and the algorithm used velocity plus position feedback ($\alpha = 1$). The input and output matrices are then

$$B_p = \begin{pmatrix} 0 \\ B_2 \end{pmatrix}$$

with

$$B_2^T = 2\begin{bmatrix} 0.790 & 0.968 & 0.397 & -0.482 \\ 0.481 & -0.844 & 0.998 & -0.905 \end{bmatrix}$$

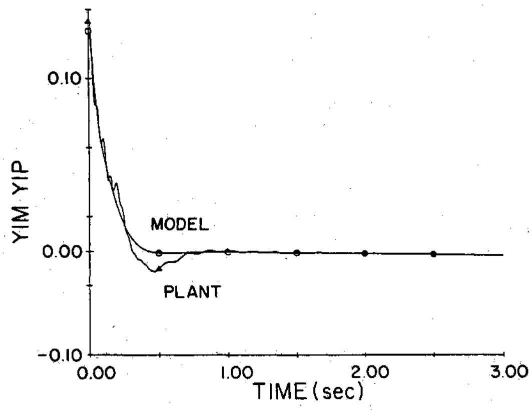

Fig. 1 Beam regulation: position outputs at first sensor.

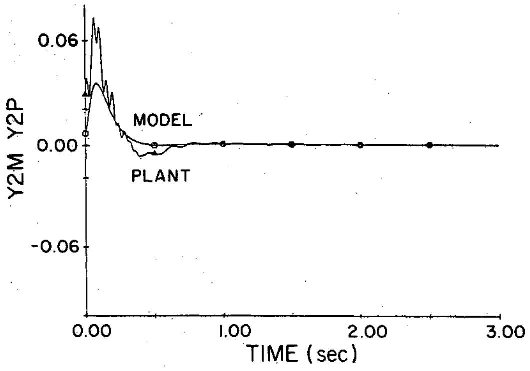

Fig. 2 Beam regulation: position outputs at second sensor.

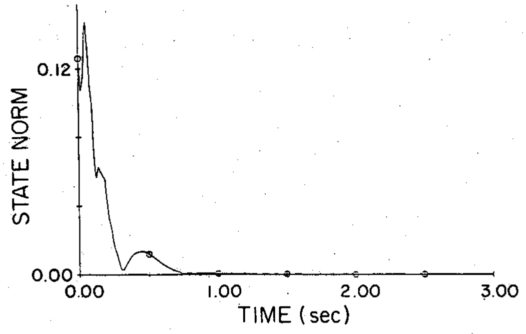

Fig. 3 Beam regulation: position state vector norm.

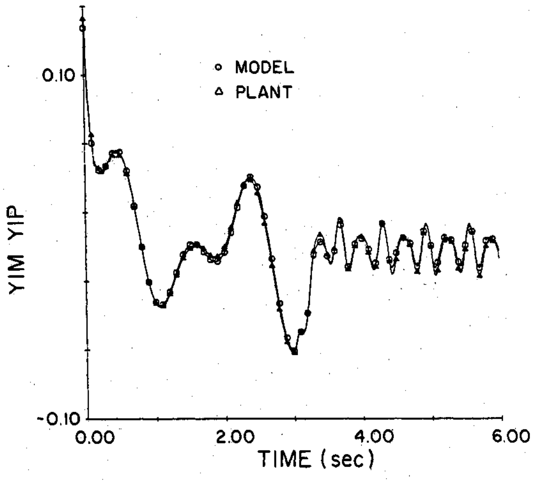

Fig. 4 Beam servo-tracking: position output at first sensor.

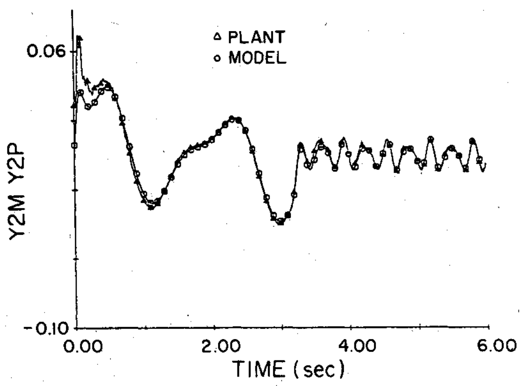

Fig. 5 Beam servo-tracking: Position output at second sensor.

and

$$C = [C_1 \; C_2] = \tfrac{1}{2}[B_2^T \; B_2^T]$$

The reference trajectories were defined by a fourth-order model containing the first two plant modes and with a damping ratio of 0.80.

The initial conditions are

$$x_p^T(0) = (0.1 \; 0.05 \; 0.05 \; 0.03 \; 0.0 \; 0.0 \; 0.0 \; 0.0)$$

and for the model

$$x_m^T(0) = (0.1 \; 0.05 \; 0.0 \; 0.0)$$

The beam was tested for both regulation and servo-following with the adaptation gain matrices T and $\bar{T}$, defined in Eqs. (14) and (15), selected as follows:

$$T = \text{diag}(100.0 \quad 100.0 \quad 10.0 \quad 10.0 \quad 10.0 \quad 10.0 \quad 4.0 \quad 4.0)$$

$$\bar{T} = \text{diag}(40.0 \quad 40.0 \quad 10.0 \quad 10.0 \quad 10.0 \quad 10.0 \quad 4.0 \quad 4.0)$$

The results of the regulation tests are represented in Figs. 1-3. The position outputs at the measuring points are represented in Figs. 1 and 2 and the position state vector norm, namely $(x_{p1}^2 + x_{p2}^2 + x_{p3}^2 + x_{p4}^2)^{1/2}$ is represented in Fig. 3. Observations show good position output following with all modes asymptotically stable.

A two-input sinusoidal command was then used for the servo-following test. The frequencies of the waves were initially 6 c/s and 4 c/s and were abruptly changed after 3 s to 30 c/s and 20 c/s. The position outputs are represented in Figs. 4 and 5 and the input commands are represented in Figs. 6 and 7. Observations show an acceptable servo-tracking, following a period of adaptation of less than 1 s. The sensors were then separated from the actuators and moved to $d_3 = 0.25$ and $d_4 = 0.76$. The corresponding matrix was

$$C_1 = C_2 = \begin{bmatrix} 0.707 & 1.0 & 0.707 & 0.253 \times 10^{-5} \\ 0.684 & -0.684 & 0.770 & -0.1253 \end{bmatrix}$$

which satisfies the relation of Eq. (23) but not necessarily of Eq. (24).

The results of the regulation test using velocity feedback only are represented in Figs. 8-10. The position outputs at sensor placements are represented in Figs. 8 and 9 and the total position state vector norm appears in Fig. 10.

The results of the regulation tests using velocity plus position feedback are represented in Figs. 11-13. The position outputs at sensor placements can be seen in Figs. 11 and 12 and the position state vector norm appears in Fig. 13.

Observations for both tests with noncollocated sensors and actuators indicate good stabilization properties although the positive realness property is only satisfied when pure velocity feedback is used.

20-State Aluminum Plate Example

An undamped 20-state (10-mode), two-output representation of a 1.5×1.5 m, 1.5-mm-thick, simply supported aluminum plate[9] was also used for regulation and control. The plate is represented by the matrices

$$\Lambda = \text{diag}(65.9 \quad 412.0 \quad 412.0 \quad 1055.0 \quad 1649.0 \quad 1649.0 \quad 2771.0 \quad 2771.0 \quad 4751.6 \quad 4751.6)$$

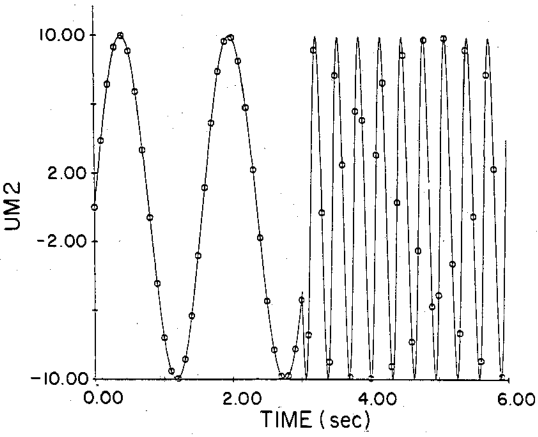

Fig. 7 Second input command.

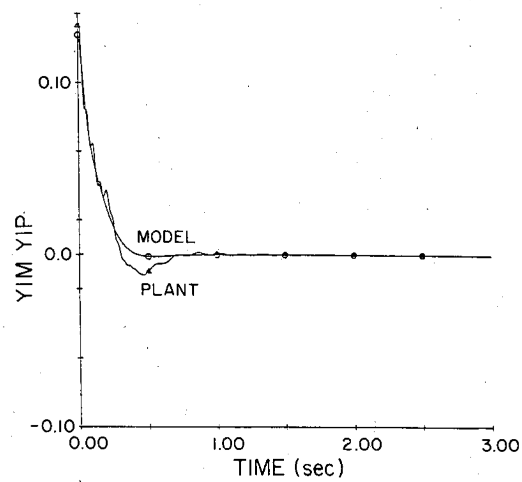

Fig. 8 Beam regulation with velocity feedback. Uncollocated sensors and actuators: position outputs at first sensor.

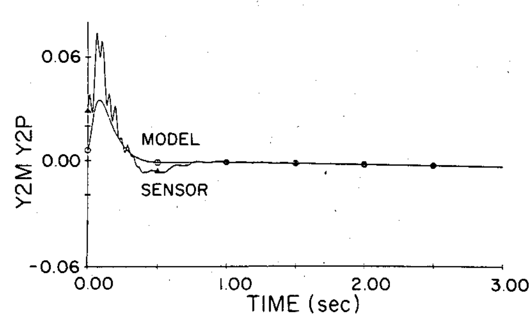

Fig. 9 Beam regulation with velocity feedback. Uncollocated sensors and actuators: position outputs at second sensor.

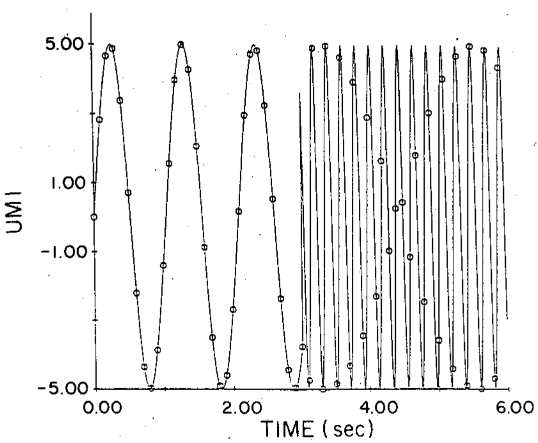

Fig. 6 First input command.

and

$$B_2^T = \begin{bmatrix} 0.326 & 0.4367 & -0.1357 & 0.1816 & -0.270 & 0.2581 & -0.107 & -0.361 \\ & & & & & & 0.248 & -0.0913 \\ 0.4246 & 0.0888 & 0.2625 & -0.0549 & -0.2625 & -0.406 & -0.250 & -0.0549 \\ & & & & & & -0.4246 & -0.1737 \end{bmatrix}$$

The reference trajectories were defined by a fourth-order model containing the first two plant modes and with a damping ratio of 0.80. The adaptation gain matrices are

$$T = (1000.0 \quad 1000.0 \quad 100.0 \quad 100.0 \quad 100.0 \quad 100.0 \quad 40.0 \quad 40.0)$$

$$\bar{T} = (100.0 \quad 100.0 \quad 10.0 \quad 10.0 \quad 10.0 \quad 10.0 \quad 4.0 \quad 4.0)$$

The position outputs at sensor placement are represented in Figs. 14 and 15 and the position state vector norm is represented in Fig. 16 for the regulation test. The results are comparable with those of Ref. 9. However, because velocity plus position feedback is now being used, it is also possible to control the final shape of the plate.

Servo-tracking of two-input sinusoidal wave, represented in Figs. 6 and 7, was also tested. The position outputs at sensor placements are represented in Figs. 17 and 18.

24-State Tetrahedral Truss Example

A 24-state (12-mode), three-output tetrahedral truss, designed by K. Soasaar and P. Strunce of the Charles Stark Draper Laboratory (CSDL), and used in Ref. 10 for Robust Control Design, is also used here as an example of a complex large structural system. However, we assume in this paper that the parameters are totally unknown and the controller is designed through the adaptive procedure of Eqs. (10-15). The truss is represented by the matrices:

$$\Lambda = \text{diag}(1.80 \quad 2.70 \quad 8.36 \quad 8.75 \quad 11.5 \quad 17.7 \quad 21.7 \quad 22.6 \quad 72.9 \quad 85.9 \quad 106.0 \quad 167.0)$$

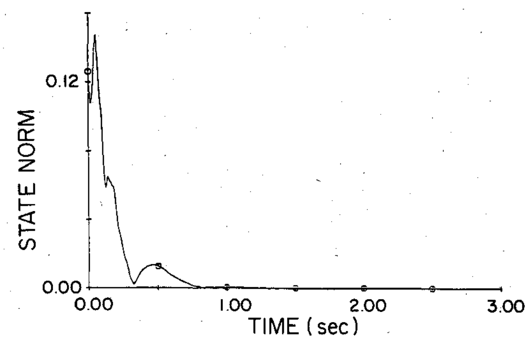

Fig. 10 Beam regulation with velocity feedback. Uncollocated sensors and actuators: position state vector norm.

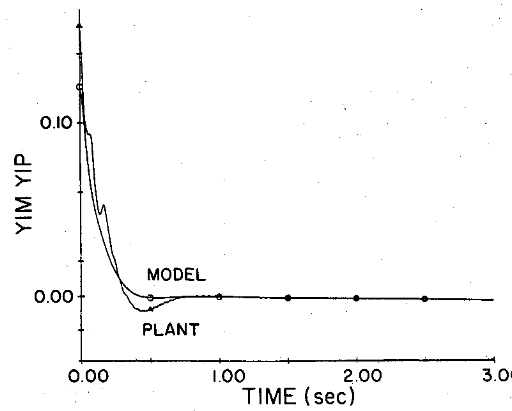

Fig. 11 Beam regulation with velocity plus position feedback. Uncollocated sensors and actuators: position output at first sensor.

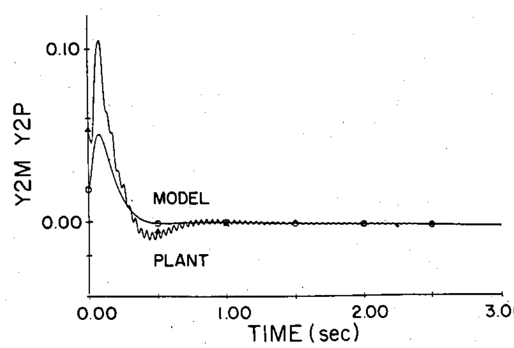

Fig. 12 Beam regulation with velocity and position feedback. Uncollocated sensors and actuators: position output at second sensor.

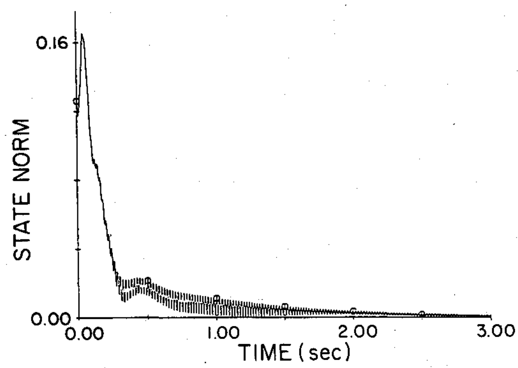

Fig. 13 Beam regulation with velocity and feedback. Uncollocated sensors and actuators: position state vector norm.

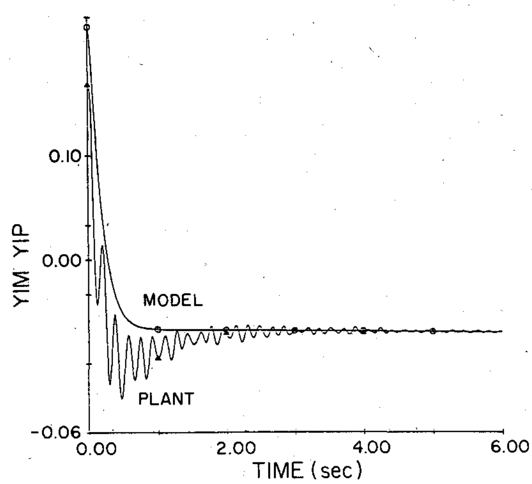

Fig. 14 Plate regulation: position output at first sensor.

$$
B_2^T = \begin{bmatrix}
-0.023 & -0.112 & 0.077 & 0.189 & 0.156 & -0.289 & -0.320 \\
 & 0.365 & -0.229 & 0.167 & -0.145 & 0.025 & \\
-0.067 & 0.017 & 0.271 & -0.050 & -0.049 & 0.289 & -0.369 \\
 & 0.299 & 0.250 & -0.150 & 0.146 & -0.013 & \\
-0.439 & 0.069 & 0.046 & -0.249 & 0.351 & -0.289 & -0.049 \\
 & -0.069 & 0.231 & -0.317 & -0.220 & 0.114 &
\end{bmatrix}
$$

The truss is forced to follow a 6-state (3-mode) reference model in three different points. The adaptation gain matrices are

$$T = [1000 \quad 1000 \quad 1000 \quad 4 \quad 4 \quad 4 \quad 4 \quad 4 \quad 4 \quad 2 \quad 2 \quad 2]$$

$$\bar{T} = [5 \quad 5 \quad 5 \quad 4 \quad 4 \quad 4 \quad 4 \quad 4 \quad 4 \quad 2 \quad 2 \quad 2]$$

Combined velocity plus position feedback is used to stabilize and control the truss.

The position outputs at sensor placements are shown in Figs. 19-21, and the position state vector norm is represented in Fig. 22 for the regulation test. The position outputs at sensor placements for the servo-control test are represented in Figs. 23-25.

The stabilization and the asymptotic model following properties of the adaptive algorithm are clear. The longer duration of the oscillations in Figs. 19 and 20, compared with Fig. 21, is due to the relative magnitude dominance of y_3 over

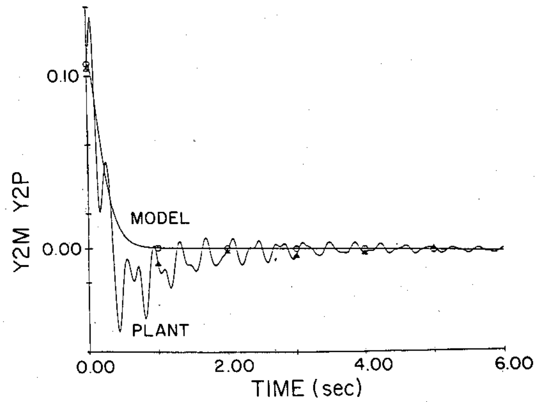

Fig. 15 Plate regulation: position output at second sensor.

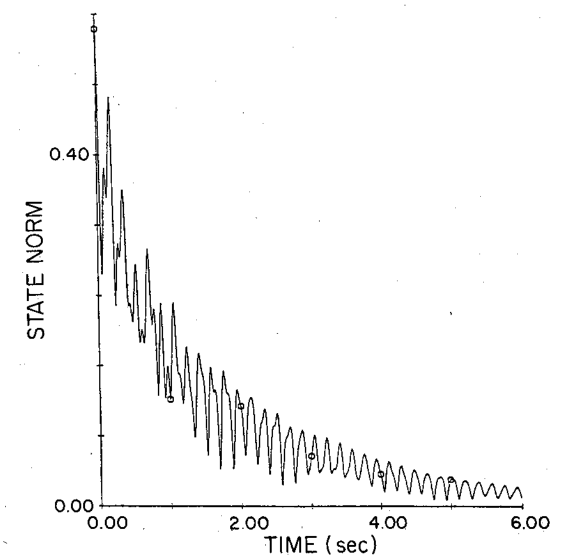

Fig. 16 Plate regulation: position state vector norm.

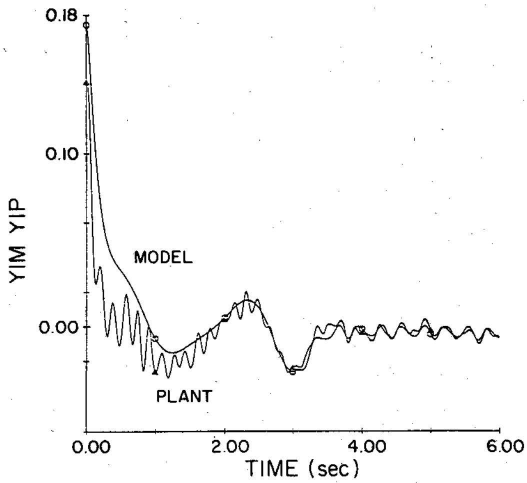

Fig. 17 Plate servo-following: position output at first sensor.

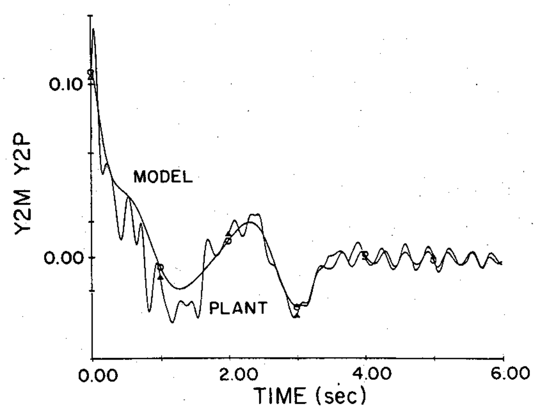

Fig. 18 Plate servo-following: position output at second sensor.

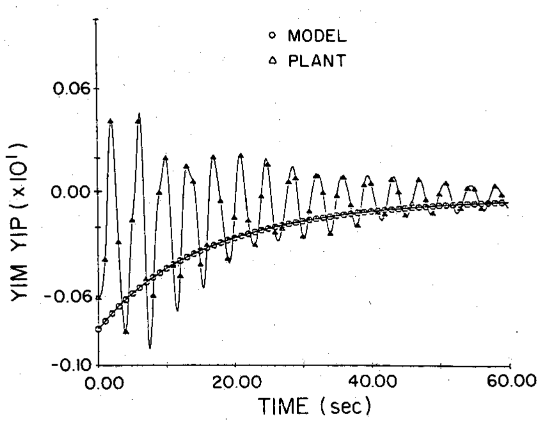

Fig. 19 Truss regulation: position output at first sensor.

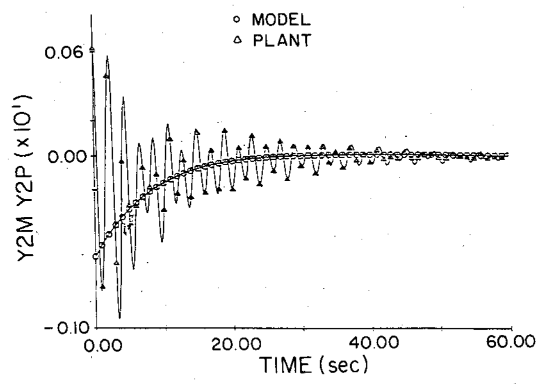

Fig. 20 Truss regulation: position output at second sensor.

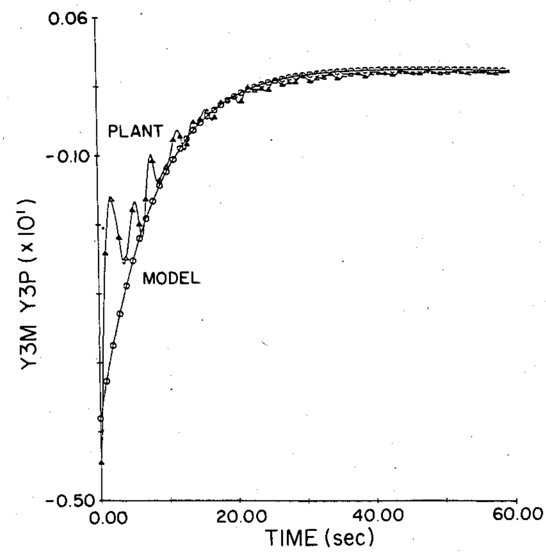

Fig. 21 Truss regulation: position output at third sensor.

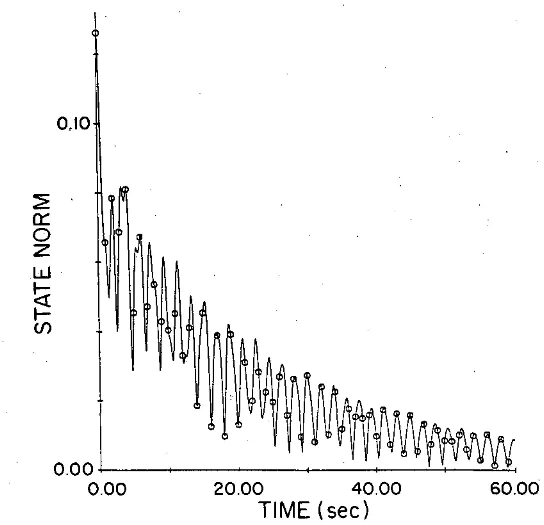

Fig. 22 Truss regulation: position state vector norm.

y_1 and y_2. In this case, the state norm which can be seen in Fig. 22 is probably more representative of the overall system performance.

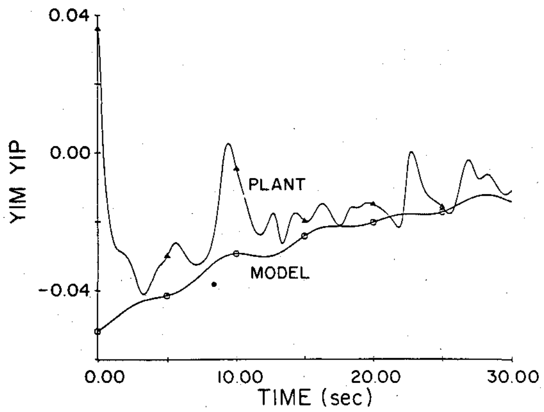

Fig. 23 Truss servo-following: position output at first sensor.

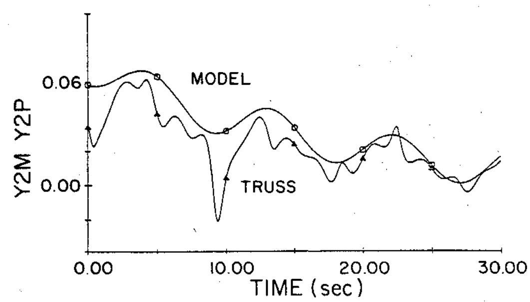

Fig. 24 Truss servo-following: position output at second sensor.

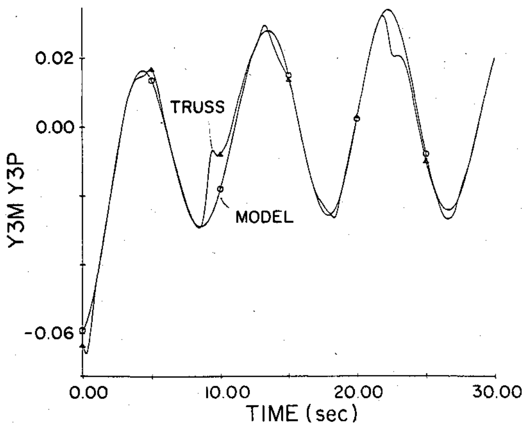

Fig. 25 Truss servo-following: position output at third sensor.

Conclusions

In this paper, direct adaptive control methods were used to design controllers for some large structural systems. The dimension of the reference model may be very small, relative to the dimension of the plant, and the implementation of the algorithm is very simple. No a priori knowledge other than the fact that the structure can be made positive real by some feedback gain (not needed for implementation). Results seem to confirm that the method has a large domain of feasibility which can be extended beyond the class of systems which satisfy the (sufficient) condition of positive realness. This property makes it possible to have both position and velocity control of LSS and also, for a limited number of modes, to control a structure, even though the sensors and the actuators are not perfectly collocated.

It should be noted that the general analytical treatment of systems with disturbances and which are output stabilizable, but not positive real, is currently under consideration. Results to date[11,12] show that for such systems a somewhat modified adaptive algorithm will give bounded input-bounded output stability with the size of the error bounds controllable with certain adaptation weighting parameters. Application of these results to more realistic large structural systems with actuator and sensor dynamics and random disturbances is currently being investigated and should be reported on in the future.

Acknowledgments

This material is based upon work supported by the National Science Foundation under Grant ECS80-16173 and by NASA under Grant NAG 1-171.

References

[1] Sobel, K., Kaufman, H. and Mabius, L., "Implicit Adaptive Control for a Class of MIMO Systems," *IEEE Transactions on Aerospace and Electronic Systems,* No. 5, Sept. 1982, pp. 576-590.

[2] Bar-Kana, I. and Kaufman, H., "Model Reference Adaptive Control for Time-Variable Input Commands," *Proceedings of the 1982 Conference on Information Sciences and Systems,* Princeton, N.J., 1982, pp. 208-211.

[3] Bar-Kana, I. and Kaufman, H., "Multivariable Direct Adaptive Control for a General Class of Time-Variable Commands," *Proceedings of the 21st IEEE Conference on Decision and Control,* Orlando, Fla., 1982, pp. 750-751.

[4] Bar-Kana, I., "Direct Multivariable Model Reference Adaptive Control with Application to Large Structural Systems," Ph.D. Thesis, Rensselaer Polytechnic Institute, Troy, N.Y., May 1983.

[5] Vidyasagar, M., *Nonlinear Systems Analysis,* Prentice-Hall, Englewood Cliffs, N.J., 1978.

[6] LaSalle, J.P., *The Stability of Dynamical Systems,* SIAM, Regional Conference Series in Applied Mathematics, Philadelphia, Pa., 1976.

[7] Bar-Kana, I., Kaufman, J., and Balas, M., "Model Reference Adaptive Control of Large Structural Systems," *Journal of Guidance, Control, and Dynamics,* Vol. 6, March-April 1983, pp. 112-118.

[8] Kaufman, H. et al., "Model Reference Adaptive Control of Large Scale Systems," *Proceedings of the 20th IEEE Conference on Decision and Control,* San Diego, Calif., Dec. 1981, pp. 984-989.

[9] Benhabib, R.J. et al., "Stability of Large Space Structure Control Systems Using Positivity Concepts," *Journal of Guidance and Control,* Vol. 4, Sept.-Oct. 1981, pp. 487-494.

[10] Arbel, A. and Gupta, N.K., "Robust Collocated Control for Large Flexible Space Structures," *Journal of Guidance and Control,* Vol. 5, Sept.-Oct. 1981, pp. 480-486.

[11] Bar-Kana, I. and Kaufman, H., "Reduced Order Model Direct Multivariable Adaptive Control," The 3rd Yale Workshop on Applications of Adaptive Systems Theory, Yale University, New Haven, Conn., June 1983.

[12] Bar-Kana, I. and Kaufman, H., "Low Order Model Reference Direct Multivariable Adaptive Control," 1984 American Control Conference, San Diego, June 1984.